

Progression of regeneration in demosponge *Cinachyrella cf cavernosa* based on wound location

Aabha Deshpande and Narsinh L. Thakur*

CSIR- National Institute of Oceanography, Dona Paula, 403004 Goa, India
Academy of Scientific and Innovative Research

*Corresponding author: email thakurn@nio.org, phone no. +91 832 240623

Conceptualisation, carrying out experiments, analysis, investigation and writing original draft:
Aabha Deshpande

Supervision, resources, review and editing the manuscript: Narsinh L. Thakur

Abstract

In this study, the differential regeneration process in sponge *Cinachyrella cf cavernosa* (Lamarck, 1815) was examined by creating wounds at basal and apical tissues. The differences in wound healing were investigated based on qualitative and quantitative changes in collagen at both wound locations. The different cell types were also documented. The basal tissue was found to heal faster than apical tissue. Collagen was 21.74% more in regenerating basal tissue than the apical tissue, indicating its involvement in accelerated regeneration. To understand the molecular process of gene regulation during regeneration in basal tissues of *C.cf cavernosa*, transcriptomic analysis was carried out using Illumina NextSeq 500. From the samples used for RNA-seq, on an average 35 million reads were obtained. Out of 65587 total Coding DNA Sequences (CDS), 37145 were annotated. The differential gene expression analysis showed up-regulation in collagen-related gene Col and actin-related genes during progressive stages of regeneration. Contrary to other metabolism-related genes, lipid metabolism related genes were expressed in more numbers with consecutive stages of regeneration highlighting their role in stress management of the sponge. This study serves to advance our understanding of the regeneration process, factors affecting the rate of this process and transcriptomic changes in regenerating sponge.

Keywords: Porifera, Tetillidae, wound healing, collagen, transcriptome

Introduction

Regeneration is not exclusive to sponges. However, the regenerative ability of sponges far surpasses that of other animals. Sponges have been reported to regenerate at a rate of 22 to 2900 times more than their growth rate (Ayling, 1983). The ecological success of sponges is most probably attributed to a rapid regeneration capacity (Van Soest et al., 2012; Alexander et al., 2015; Ereskovsky et al., 2017b). They are capable of wound healing, body part regeneration, the formation of primmorphs (3D cell aggregates), and entire functional bodies from dissociated cells (Lavrov and Kosevich, 2014, 2016; Ereskovsky et al., 2017a, b). These factors make sponges a key model to understand the evolutionary history of regeneration in animals. Regeneration is also used for biomass production in some species (Coutinho et al., 2017). It involves different processes like cell migration, dedifferentiation, and transdifferentiation (Ereskovsky et al. 2015, 2017a, b, 2019; Borisenko et al. 2015; Lavrov et al. 2018). These processes involve different components, most notably collagen (Alexander et al., 2015), archaeocytes, and choanocytes (Ereskovsky et al. 2015; Borisenko et al. 2015; Lavrov et al. 2018), and growth factors like TGF (Pozzolini et al. 2019).

Collagens, the structural proteins found in the extracellular matrix have various functions including a structural function in cartilage (Responde et al. 2007) and skin formation (Raine-Fenning et al. 2003), biomineralisation of hard tissues, and the regulation of diverse cellular functions and processes (Ehrlich et al., 2018). As a structural protein, collagen participates in wound healing and regeneration (Alexander et al., 2015). Cellular mechanisms are equally important for regeneration. Archeocytes, known for their pluripotency, appear to be a part of the regeneration process in Demosongiae. Many of the cells in newly formed regions share features with archaeocytes. Hence, they are thought to be of archaeocyte origin (Simpson, 1984). The presence of choanocytes through different stages of regeneration was reported in a few studies. Choanocytes may be transdifferentiating during regeneration in sponges (Ereskovsky et al. 2015, 2019; Borisenko et al. 2015; Lavrov et al. 2018).

Various factors, intrinsic and extrinsic, affect regeneration in sponges. Henry and Hart (2005) have reviewed regeneration in sponges and corals and infer that the regenerative capacity of these animals depends on the location of the wound. Wulff (2010) state that along with the location of the wound, amount of damage, type of damage, the size of the sponge can affect the recovery of the sponge. Previous studies have described the regeneration in different sponge species based on wound size (Sheild and Whitman, 1993; Schmahl, 1999) and growth forms (Reiswig, 1973; Wilkinson and Thompson, 1997). Nevertheless, there is a lack of studies based on the location of the wound in the same species of sponge. The basic information on regeneration in sponges from the Indo-Pacific region is also unavailable (Singh and Thakur, 2016). Hence, we decided to study regeneration at

different wound locations in a globular sponge *Cinachyrella cf cavernosa* (Lamarck, 1815) abundantly found on the Indian coast.

Sponges, even though evolutionarily significant, have long been ignored when it comes to genomic and transcriptomic studies. This picture is slowly changing with the advent of next generation sequencing (NGS) technologies. There are reports of gene expression studies carried out in sponges for evolutionary and phylogenetic analysis (Larroux et al., 2006; Riesgo et al., 2014a), development studies (Riesgo et al., 2012), novel species description (Ereskovsky et al., 2017c), life cycle stages elucidation (Conaco et al., 2012; Perez-Porro et al., 2013; Qiu et al., 2015), host- symbionts relation (Riesgo et al., 2014b), specific processes like biomineralisation and spicule formation (Voigt et al., 2017), the effect of stress factors (Guzman and Conaco, 2016), and response to grafting (Grice and Degnan, 2017). Most recently, Kenny et al. (2018) have published a transcriptomic study of regeneration in *Halisarca caerulea* Vacelet and Donade, 1987. In the current study, we investigate gene expression in different stages of regeneration on *C. cf cavernosa* using transcriptome.

C. cf cavernosa is tetillid sponge found in the inter-tidal area. This golf ball sponge has been studied for growth and regeneration under the influence of competition (Singh and Thakur, 2016). The authors reported 50-100 times faster regeneration in this sponge compared to its average growth rate.

In the current study, we have examined the difference in the rate of regeneration based on location (basal tissue and apical tissue) of experimentally inflicted wounds. We also studied this difference concerning collagen during regeneration and documented different cell types. Lastly, we studied the transcript in the sponge based on stages of regeneration.

Materials and Methods

Collection of sponges

Live specimens of intertidal marine sponge *Cinachyrella cf cavernosa* (Tetillidae, Demospongiae) were collected from Mhapan, central west coast of India (15°55'25" N, 73°33'16" E) during low tide (ambient temperature 29°C), transported to the laboratory in well-aerated seawater. The sponges were acclimatised for two weeks in natural seawater at room temperature and were fed twice a week. The sponges were fed a home-grown pure culture of *Chlorella* sp. Large aquarium (~ 100L volume) was used to house all the sponges together during acclimatisation. Sponges of the same size (approximately 4 cm in diameter) were used for the experiment.

Experimental design

Acclimatised sponges in triplets were transferred to smaller aquaria (~25L volume) for the experiment. To ascertain the difference between wound healing at the basal tissue and apical tissue, six sponges were inflicted with artificial wounds in basal tissue and another six in apical tissue. The scheme of wound locations is explained in Fig. 1. The wounds were created with a sterile scalpel and were modelled after nudibranch bites observed in the field. All the wounds were kept uniform (average depth 0.4 cm, average surface area 20 cm², and no more than 10% of the total volume of sponge) to avoid bias from wound size. The entire experiment with replicates was repeated three times. The wound healing pattern was determined based on measurements of wounds (mm³) and photographs taken every day for each of the sponges. The volume of the wound was calculated using the elliptical cone as a model. Tissue samples from each group were collected thrice, at the start of the experiment, during regeneration (the seventh day after wound infliction) and after regeneration (15-20 days after wound infliction). These samples were analysed for histology, cell types and transcriptomic changes.

Qualitative analysis of collagen

Sampled sponge tissue for histological analysis was preserved in 4% formalin diluted with seawater. These samples were treated with 10% hydrofluoric acid for eight hours at 4°C to remove spicules and sand particles and dehydrated through graded ethanol series. After washing with 100% ethanol twice, the samples were treated with Benzene and transferred to Paraffin wax (Sigma-Aldrich, Germany catalogue no. 327212). After three changes of wax for better incorporation, tissues were cast in paraffin wax blocks. Trimmed wax blocks were mounted on Leica RM 2125 RTS microtome and sectioned. For detection of collagen, these sections were stained with Picro-Sirius red (Puchtler et al., 1973; Alexander et al., 2015). In short, the wax was removed with Xylene and rehydrated through graded ethanol series up to distilled water. Slides were incubated in 0.2% phosphomolybdic acid for 5 minutes and stained with 0.1% picrosirius red for 60 minutes. Sections were dehydrated in ethanol and xylene and mounted in DPX. Sections were visualised and photographed under cross-polarised light using a Nikon LV100 microscope.

Quantification of collagen

Collagen was extracted according to Dieht-Seifert et al. (1985) and Swatschek et al. (2002) from three groups of samples viz., before wound infliction, i.e. control, regenerating basal tissue and regenerating apical tissue. Each sponge containing either basal or apical injury was processed separately to ascertain the effect of site of injury on collagen content. Sponges were cut into small

pieces and homogenised in 100mM Tris-HCl buffer containing 10mM EDTA, 8M urea, and 100mM 2-Mercaptoethanol (pH 9.5). Sodium hydroxide was used to raise the pH of this solution to 9, and it was stirred for 24 hours at room temperature. This viscous extract was centrifuged for 5 minutes at 5000g and 2°C. The supernatant was used to precipitate collagen by adjusting pH to 4 with acetic acid. This solution was centrifuged for 30 minutes at 20000g at 2°C. The pellet was washed with distilled water and centrifuged under the same condition. The resulting pellet was lyophilised and weighed for gravimetric analysis.

Analysis of cellular content in regenerating tissue of the sponge

Tissue samples were preserved in 4% glutaraldehyde diluted with sodium cacodylate buffer for a minimum of three days. The samples were treated with 4% Hydrogen Fluoride for two hours at room temperature, washed with 0.2M sodium cacodylate buffer (pH 7.4), and incubated in 1% Osmium tetroxide overnight at 4°C. Tissue samples were rewashed (3-4 times) with sodium cacodylate buffer by repeated centrifugation and further taken for dehydration through graded ethanol series. ARALDITE/Embed embedding kit (Electron Microscopy Sciences) was used according to the manufacturer's instructions for casting the blocks. Cryo-ultraMicrotome (RMC) was used for sectioning. These thin sections were stained with 2% aqueous Uranyl acetate and 0.04% lead citrate. The sections were visualised using FEI Technai T12 G2 Spirit Transmission Electron Microscope at 70kV.

RNA extraction, library preparation, and sequencing

Based on wound healing pattern, we decided to use basal tissue (which was healing faster) for transcriptomic analysis and samples (no replicates) from the tissue before wound infliction, during regeneration, and completely regenerated tissue each were used. Tissue samples were flash-frozen with liquid nitrogen and stored at -80°C. Total RNA was isolated using the traditional TRIzol method. The quality and quantity of RNA were checked on 1% denaturing RNA agarose gel and NanoDrop. The RNA-Seq paired-end sequencing libraries were prepared using IlluminaTruSeq stranded mRNA sample prep kit using the manufacturer's instructions. The PCR enriched libraries were analysed in 4200 Tape Station system (Agilent Biotechnologies) using high sensitivity D5000 Screen tape according to manufacturer's instructions. After quality and quantity check, the PE Illumina libraries were loaded onto NexSeq 500. The kit reagents were used in the binding of samples to complimentary adapter oligos on the paired-end flow cell. The adapters were designed to allow selective cleavage of the forward strand during sequencing. The copied reverse strands then used to sequence from the opposite end of the fragment. All the sequences are deposited in NCBI's

Gene Expression Omnibus (Edgar et al., 2002) and can be accessed with GSE134724 (<https://www.ncbi.nlm.nih.gov/geo/query/acc.cgi?acc=GSE134724>).

De novo transcriptome assembly

The sequenced raw data were trimmed to obtain high quality, clean reads using Trimmomatic v0.35 (Bolger et al., 2014). Adapter sequences, ambiguous reads (reads with unknown nucleotides “N” larger than 5%), and low-quality sequences (based on Phred score) were eliminated. Minimum length of 50 nucleotides was applied. Due to unavailability of the genome of *C. cf cavernosa*, the high quality, paired-end reads were used for De novo assembly. The reads of all the samples were pooled and assembled into transcripts using Trinity v2.5.1 (Grabherr et al., 2011) with k-mer of 25. Minimum contig length of 200bp was maintained to avoid poor similarities (Riesgo et al., 2012). The transcripts were clustered in unigenes based global sequence identity threshold of 90% using CD-HIT-EST v 4.6 (Li and Godzik 2006) to reduce redundancy. RSEM v 1.2.31 (Li and Dewey 2011) was used to compute abundances based on mapping of pooled high quality reads to the predicted Unigenes via Bowtie2 v 2.2.6. Unigenes with 3x read depth and 80% coverage were considered for further analysis. BUSCO was run against eukaryota_odb9 and metazoa_odb9 to determine the completeness of the transcriptome.

Gene annotation and differential analysis

The TransDecoder v2.0 was used to predict coding sequences. These CDS (Coding DNA Sequence) were quantified based on mapping of sample-wise high quality reads to the pooled CDS via RSEM and SAMtools. CDS were searched against the NCBI nr database using DIAMOND (Buchfink et al., 2015) with E-value cut-off $1e^{-5}$. CDS were identified in each sample based on 2x read depth and 50% coverage.

Gene ontology annotations of coding sequences were determined using the Blast2GO programme. Ontology assignments were used to classify functions of the predicted CDS. The gene product properties were derived from GO mapping. These properties were divided into three main domains, viz., biological processes, molecular functions, and cellular components. BLASTX was used to functionally annotate CDS and GO mapping was carried out to retrieve GO terms. The distribution GO terms across three domains mentioned earlier was carried out using WEGO and Blast2GO (Goetz et al., 2008).

CDS were mapped to reference canonical pathways in KEGG to identify their potential involvement in biological pathways. The KEGG Orthology database of *Amphimedon queenslandica* Hooper & van Soest, 2006 was used as the reference for pathway mapping. All the CDS were classified under

five main categories, metabolism, cellular processes, genetic information processing, environmental information processing, and organismal systems. KAAS (KEGG Automated Annotation Server), which includes KEGG Orthology assignments with corresponding enzyme commission and metabolic pathways of predicted CDS, was used to process identified CDS in different samples. These CDS were categorised in different functional pathway categories and annotated by KAAS (Moriya et al., 2007).

Differential gene expression analysis was performed on CDS common between a pair of samples at a time by employing a negative binomial distribution model in DESeq package v1.22.1 (Anders and Huber, 2010). Dispersion values were estimated with the following parameters: method – blind, sharing Mode – fit-only, and fit type– local. The Log₂ Fold Change (FC) value was calculated on the read abundance. The CDS with FC value greater than zero were considered up-regulated, and less than zero was considered down-regulated. CDS with a p-value threshold of 0.05 were considered statistically significant. A complete linkage hierarchical cluster analysis was performed on top 60 differentially expressed CDS using Multiple Experiment Viewer v 4.8.1 (Howe et al., 2011). Heat maps were constructed using log-transformed and the normalised value of CDS, based on Pearson un-centred correlation distance and complete linkage method.

Results

Cinachyrella cf cavernosa is a globular tetillid sponge. The tissue of this sponge is dense and has bundles of spicules radiating from roughly the centre of the sponge. The ectosome and choanosome can be differentiated based on the presence of cells and an abundance of collagen. Choanosomes show most of the cells and the presence of choanocyte chambers, whereas ectosome shows densely packed collagen fibres.

Wound healing pattern

In the current study, the entire duration of regeneration was recorded until the lost biomass was recovered. The samples were taken over a more extended period. The stages of regeneration were defined over the scale of days. The samples were taken on day 0 (before wound infliction), day 7 (during regeneration, half-way mark for regeneration), and completion of regeneration. The individual variation in the rates of regeneration was observed in the sponges, as the ones with basal wounds regenerated faster than sponges with apical wounds. The volume of the wound was recorded from infliction to complete regeneration; the average was taken for each group and converted into a percentage to show the pattern of wound healing. The initial phase of healing was rapid (Figure 2). By the seventh day, 90% of basal wounds and 72% of apical wounds were healed. The damaged area

was measured every day until the sampling or complete regeneration in individual cases. By the tenth day, all the sponges with basal wounds had regenerated entirely except for a small depression. The rate of regeneration in sponges with apical wounds fell further after the tenth day. All the sponges with apical wounds were entirely regenerated by the twentieth day.

Qualitative and quantitative analysis of collagen

Figure 3A shows the progression of regeneration in basal tissue of *C. cf cavernosa*. The photos are taken on day 0 (before wound infliction), day 7 (during regeneration), and day 10 (complete regeneration). The second row shows corresponding tissue sections of sponges stained with Picro-Sirius red under bright light and the third row shows the same sections under polarised light. Figure 3B shows the corresponding images for the apical tissue of the sponge. Staining with Picro-Sirius red revealed a high abundance of collagen in the cortical region of the sponge. The canals and spicule bundles were seen to be lined with collagen as well. These features were observed irrespective of the location of the sample. Use of cross-polarization filters further clarified the situation. Under this filter, two types of collagen fibres were observed, viz., thin (green in colour) and thick (orange in colour). The centre of this globular sponge, which is known to be originating point of radiating spicule bundles, was rich in collagen, specifically in thick collagen. Sections from basal tissue at each of the stage of regeneration showed more collagen and brightly lit section when compared to the apical section at the respective stage. The thicker collagen (orange in colour) was more abundant in basal sections than in apical sections.

Changes in collagen were also examined using TEM (Figure 4). Figure 4a and 4c show control tissue of basal and apical part of the sponge, respectively. Both these photos show densely and uniformly distributed collagen. In basal tissue, the collagen can be seen more prominently. During regeneration on day 7, clumps on collagen can be seen starting to form in basal (Figure 4b) as well as apical tissue (Figure 4e). At the completion of regeneration, in basal tissue (Figure 4c) clumps of collagen can be seen among threads of collagen. Such clumps of collagen are more prominently seen in apical tissue at the completion of regeneration (Figure 4f).

The weight of collagen, extracted from each specimen, was converted into a percentage of total body weight of sponges. The results clearly showed the lowest quantity of collagen (1.2%) present in non-regenerative tissue (Figure 5). A higher quantity of collagen (2.3%) was seen in regenerative apical tissue, and the highest collagen quantity (2.8%) was seen in regenerative basal tissue.

Analysis of cellular contents in regenerating tissue of the sponge

In TEM analysis of regenerating sponge tissues, different cell types were observed, including collencytes, which secrete collagen (Figure 6d). Archaeocytes (Figure 6a) and cells with inclusions (Figure 6e) were observed. The choanosomes and constituent choanocytes were also observed (Figure 6b). In the regenerating tissue (sample taken on day seven during regeneration), we observed elongated migrating cells, all arranged along the same axis (Figure 6f, Figure 4b and 4e). We have also seen empty cells in regenerating tissue (Figure 4f). We cannot ascertain if different cell types are responsible for the difference in the rate of regeneration between basal and apical wounds. However, we repeatedly observed collagen fibres. Two types of collagen fibres were observed, one was haphazardly arranged and the other well structured. Canals and spicule bundles were lined with thick collagen. These observations are consistent with histological analysis

Gene expression analysis

Cinachyrella cf cavernosa was inflicted with wounds in laboratory aquaria, and transcriptome was studied at three stages viz., before wound infliction, during regeneration, and after regeneration. Sequences with less than 20 Phred score were trimmed along with adapter sequences, and ambiguous sequences (reads with the number of unknown nucleotides larger than 5%). After cleaning, the GC content of sequences was reasonably constant, with 49.5% for the sample before wound infliction, 50.5% for the regenerating sample, and 50% for the completely regenerated sample.

We obtained 33,620,431 reads for assembly A (before wound infliction), 35,636,884 reads for assembly B (during regeneration), and 37,688,551 reads for assembly C (complete regeneration). These high-quality reads were pooled and assembled into transcript using Trinity v2.5. The transcripts were clustered in Unigenes using CD-HIT-EST. We report more than 96 million base pairs in Unigene length and total 102,443 Unigenes. 33,985 Unigenes were longer than 1000bp. The N50 value was 1032, and it was comparable to previous studies (Riesgo et al., 2014a; Kenny et al., 2018). These parameters indicate good quality assembly. BUSCO was run against eukaryota_odb9. The results showed 98.7% complete BUSCOs, zero missing and four fragmented BUSCOs. BUSCO was also run against metazoan_odb9. Total 978 BUSCO groups were searched with 94.1% complete BUSCOs, 2.8% missing and 3.1% fragmented BUSCOs. These BUSCO scores indicate sufficient depth of transcriptome.

The Unigenes were validated using RSEM, and coding sequences were predicted using TransDecoder. We predict 65,587 CDS with a total length of more than 57 million bp. A total of 18,585 CDS were longer than 1000bp with an N50 value of 1062. The predicted CDS, when

searched against the NCBI non-redundant protein database, resulted in the annotation of 37,145 CDS. Assembly-wise CDS information is summarised in table 1.

Further, Gene Ontology annotations of these CDS were obtained. The predicted CDS were mapped on reference canonical pathways in KEGG (Kyoto Encyclopaedia of genes and genomes) to identify their potential involvement in biological pathways. All the CDS were categorised in five categories viz., Metabolism, Cellular processes, Genetic information processing, Environmental information processing, and Organismal system (Online Resource 1). The KEGG pathway classification was compared among the three samples. The maximum number of genes in most of the categories was seen in the control sample, i.e. before wound infliction. A dip in the number of genes expressed was observed during regeneration followed by a resurgence in the completely regenerated tissue sample. The contradictory trend was observed in a handful of categories. Genes related to lipid metabolism showed an increase in the number of genes with the progress of regeneration. A similar trend was also observed in genes involved in glycan biosynthesis and metabolism, metabolism of terpenoids and polyketides, and biosynthesis of secondary metabolites.

Differential gene expression analysis was performed on CDS common amongst all three samples. Up-regulation and down-regulation were decided based on log₂ fold change value. Between the control sample and tissue sample collected during regeneration, 963 CDS were commonly expressed, out of which 252 were up-regulated, and 216 were down-regulated. Between control and completely regenerated sample, 1320 CDS were found common. This number is in keeping with the general trend of the number of genes observed, as explained previously. Out of the commonly observed CDS, 210 were up-regulated, and 218 were down-regulated. In the last pair of samples taken during regeneration and after complete regeneration, 1199 CDS were commonly observed, out of which 196 were up-regulated, and 234 were down-regulated. We also compared the up-regulated and down-regulated genes between three sample pairs, 1) control sample and sample during regeneration, 2) control sample and completely regenerated sample, and 3) sample during regeneration and completely regenerated sample. The top ten up-regulated and down-regulated genes for all three pairs are listed in table 2.

Discussion

Regeneration in sponges is a highly variable process. Hence, its pattern cannot be predicted by the phylogenetic position of the sponge alone but is influenced by a plethora of intrinsic and extrinsic factors (Wulff, 2010). The intrinsic factors include size, age, morphology, genotype (Henry and Hart, 2005), and structural complexity (Wulff, 2006). Singh and Thakur (2016) reported that smaller

individuals of *Cinachyrella cf cavernosa* regenerate faster than the larger individuals. Sponges of similar size (approximately 4 cm in diameter) were included in the present study to avoid such bias. The inherent complexity of the structure of an organism inversely affects its ability to regenerate (Wulff, 2006). Increased regeneration rate in *C. cf cavernosa*, i.e. 50-100 times faster than the growth rate, is considered the result of structural homogeneity (Singh and Thakur, 2016).

From the literature, the regeneration duration for demosponges seems to be three days to two weeks (Borisenko et al., 2015; Ereskovsky et al., 2019). Wulff (2010) present the regeneration rate of thirteen sponges of different growth forms. *Tedania klausii* Wulff, 2006 (massive, tall mounds) and *Biemna caribea* Pulitzer-Finali, 1986 (branches, tubes, and encrusting forms) had shortest regeneration duration (~ 6 days) while *Tedania ignis* (Duchassaing & Michelotti, 1864; massive, rounded mounds) and *Haliclona implexiformis* (Hechtel, 1965; massive rounded mounds) had most prolonged regeneration duration (> 18 days). For *C. cf cavernosa* which has solitary individuals and spherical growth form, this duration is 15 days on an average.

Wound characteristics, including wound size, affect the regeneration capacity and consequently the survival of the organism. Different wound sizes are seen in different species of sponges as a result of natural or anthropological activities. The wounds range from small-scale predatory marks of nudibranchs (personal observations), trunkfish bites (Wulff, 2010), Hawksbill turtles (Pawlik et al., 2017) to large-scale destruction by bottom trawlers and storms (Henry and Hart, 2005). Henry and Hart (2005) also report a linear decrease in regeneration rate with the increase in wound size. As the sponge *C. cf cavernosa*, is an intertidal sponge, bottom trawlers do not affect it. This globular sponge rarely faces extensive damage. However, we have observed nudibranchs and gobi fishes preying on the sponges. Therefore, we limited the size of the wounds similar to predatory marks which did not exceed 10% of the total volume of the sponge.

Wound location is another wound characteristic studied in sponges. In *Mycale laxissima* (Duchassaing & Michelotti, 1864), stalks broken during a storm could not reattach (Reiswig, 1973). Similarly, in finger-shaped sponge *Isodictya* sp., the wounds caused by starfish feeding were studied, and it was found that wounds at the base of the sponge caused breakage during storms (Shield and Witman, 1993). *Neofibularia nolitangere* (Duchassaing & Michelotti, 1864), a vase-shaped sponge, healed quickly when experimentally wounded at the top of the sponge compared to the lateral side of the sponge. However, in *Ircinia strobilina* (Lamarck, 1816), the wounds on the lateral surface healed quicker than wounds on top of the individuals (Hoppe, 1988). In an extensive study conducted by Wilkinson and Thompson (1997), it was found that sponges with stalked forms and flattened forms could not reattach in a transplant experiment. The previous reports illustrate the success or failure of

regeneration based on the wound location. In the current study, we investigate the effect of wound location on the rate of regeneration in the sponge and the reasons behind it. To check the effect of wound location on *C. cf cavernosa*, we experimentally inflicted wounds on its basal part (attaches to a substratum) and apical part (diametrically opposite). Our results clearly show the faster regeneration in the basal part of the sponge. This increased rate of regeneration may be a result of the availability of energetic and cellular resources. To elucidate the difference, if any, between basal and apical tissue, we decided to investigate collagen content and types of cells occurring in these tissues.

Alexander et al. (2015) have reported a high abundance of collagen fibres in regenerative tissue in *Halisarca caerulea*, while another Keratose sponge *Chondrosia reniformis* Nardo, 1847 showed an opposite trend where collagen content has reduced and collagen gene expression down-regulated (Pozzolini et al. 2019). In the current study, we showed an increase in the collagen content of regenerating tissue of the sponge *C. cf cavernosa*. We also showed the difference in collagen content between basal and apical tissue. In the two control samples, i.e. before wound infliction, the collagen content was higher in basal tissue as compared to apical tissue. Similar observations were made through the consequent regenerative stages (Figure 3 and 4). We also show more abundance of thick collagen, i.e. type I collagen (Pozzolini et al. 2019) in basal tissue as compared to apical tissue. These two factors together may contribute to the increased rate of healing in the basal tissue of *C. cf cavernosa*.

Regeneration is a common phenomenon in metazoans. In many cases, stem cells proliferate during regeneration. Some organisms even maintain a pool of stem cells (Alexander et al., 2015). In the case of demosponges, archaeocytes are the pluripotent cells. Archaeocytes are found in the mesohyl. They are characterised by the nucleolate nucleus and may also exhibit phagosome and pseudopodia (Simpson, 1984). We investigated basal and apical tissue in different stages of regeneration for the presence of archaeocytes. The other cell types which may be participating in regeneration are choanocytes by way of transdifferentiation (Ereskovsky et al., 2015, 2017b, 2019; Borisenko et al., 2015; Lavrov et al., 2018). Choanocytes are well-defined cells with flagella and collar of microvilli. They are smaller than archaeocytes with an average size of 5-10µm in *C. cf cavernosa*. We identified choanocytes in all the tissue samples, experimental as well as control.

With the histological and gravimetric analysis, we have shown the positive involvement of collagen in accelerated regeneration in a specific part of the sponge. We also observed migrating cells in regenerating tissue. After satisfactorily establishing the difference in the rate of regeneration, we moved towards gene expression analysis of regeneration, this time using fast regenerating tissue in the basal part of the sponge.

The first complete genome of a sponge was published in 2010 (Srivastava et al., 2010) for a demosponge *Amphimedon queenslandica*. *Tethya wilhelma* Sarà, Sarà, Nickel & Brümmer, 2001 is only the second demosponge to have complete genome sequenced (Francis et al., 2017). Spongebase.net (www.spongebase.net) also reports the availability of genome of *Oscarella pearsei* Ereskovsky, Richter, Lavrov, Schippers & Nichols, 2017, a homoscleromorph, as published by Nichols et al. (2012) and *Sycon ciliatum* (Fabricius, 1780), a calcareous sponge as published by Fortunato et al. (2014). These genomes compared to 9245 extant species of sponges (according to World Porifera Database), are not even representative of all classes.

In the current investigation, we could report 102,443 Unigenes and 65,587 CDS. Out of all these, we got BLAST hits only for 37,145 CDS (56.6% of the total CDS). A reason for this could be the lack of information on sponge genomes. As stated by Renard et al. in their 2018 review, less annotation seems to be a common problem in non-model organisms, including sponges. They suggest the reason to be the difficulty automated annotation procedures have with divergent sequences. We have found 42.5% genes similar between *C.cf cavernosa* and *A. queenslandica*. Francis et al. (2017) have reported 57% identity between *A. queenslandica* and *T. wilhelma*. The average identity between different sponges is estimated to be 57.8%, which could be another reason for the lack of annotations (Renard et al., 2018).

We mapped the annotated CDS to reference canonical pathways in KEGG. In most pathway categories, the number of genes expressed before wound infliction was highest. The number reduced during regeneration and increased again with the completion of regeneration. This dip in the number of genes associated with various functional pathways of metabolism, genetic information processing, and cellular processes could be because of the shift of focus from homeostasis maintenance to wound healing. An opposite pattern is observed in genes related to lipid metabolism. Genes like stAR related lipid transfer protein, Propionyl-CoA carboxylase protein were seen to be up-regulated in during regeneration and with complete regeneration, as compared to control sample, underlining the role of lipids in sponge stress response. Benette et al. (2017) showed that sponge lipid and fatty acids might play an essential role in its response to increased temperatures. Lipids and fatty acids are part of the sponge stress response and survival under changing climate conditions. Here, we show an increased expression of genes related to lipid metabolism, possibly as a response to stress induced by wounds.

Our results of histological analysis have shown the involvement of collagen in wound healing and regeneration. Hence, we focused on collagen-related genes in differential gene expression analysis. We observed up-regulation of Col protein in the completely regenerated sponge as compared to

sponge during regeneration. Other structural proteins, like actin, could also play an important part in wound healing. Actin-related proteins are also involved in cell mobility which is essential for regeneration (Lavrov et al., 2018). We have observed up-regulation in several actin-related genes (alpha-actinin, beta-actin, gelsolin, etc.) and speculated their involvement in regeneration in sponges. A study on *C. reniformis* focuses on the TGF- β pathway and superfamily member genes (Pozzolini et al. 2019). The authors confirm the involvement of TGF superfamily genes in early regeneration. However, the authors also show involvement of superfamily members in down-regulating/inhibiting collagen expression and as a result, a decrease in collagen quantity in regenerating tissue of the sponge. This result is contradictory to the trend observed in higher animals where TGF genes promote fibrogenesis. Our results are in agreement with the general trend. Even though we cannot comment on the involvement of TGF- β pathway, we show a definite increase in the production of collagen in regenerating sponges. We also suggest an in-depth targeted approach to check the expression of genes as a prospect for sponge regeneration.

Conclusion

Cinachyrella cf cavernosa is a slow-growing sponge with high regeneration capacity. The wounds at the basal part of the sponge heal twice as fast as the wounds at the apical part. The basal tissue was found to contain 21.74% more collagen as compared to the apical tissue, indicating the involvement of collagen in accelerated regeneration. This trend was observed in the gene expression pattern, as well. Collagen-related genes and other structural elements like actin-related genes showed up-regulation in regenerating samples and in the completely regenerated sample. We observed the presence of archaeocyte, choanocyte, and collencyte, among other cell types. The up-regulation of lipid metabolism-related genes underlines their role in stress management in sponges. The results underline the importance of collagen in the early stages of wound healing. This study sheds light on the regeneration process in one of the earliest metazoans at various levels, which may be useful in regenerative medicines.

Acknowledgements

Authors thank the Director, CSIR-NIO for providing infrastructure facilities. We thank Dr Abhishek Saha for providing a polarised light microscope, Mr Azraj Dahihande for invaluable help in sample collection and laboratory experiments, and Mr Shriraj Jakhalekar for identification of cell types. We would also like to thank Dr Nagendra Singh of the National Centre for Biological Sciences and CCAMP for making TEM facility available. A.D. thanks Council of Scientific and Industrial Research for a research fellowship. Both authors acknowledge and appreciate the comments given by

anonymous reviewers. This work was partially supported by Council of Scientific and Industrial Research funded project ‘Ocean Finder’ (PSC0105) and is NIO contribution.....

Conflict of Interest: The authors declare that they have no conflict of interest.

References

1. Alexander, B.E., M. Achlatis, R. Osinga, H.G. van der Geest, J.P.M. Cleutjens, B. Schutte & J.M. de Goeij, 2015. Cell kinetics during regeneration in the sponge *Halisarca caerulea*: how local is the response to tissue damage? PeerJ 3: e820, doi: 10.7717/peerj.820
2. Andres, S. & W. Huber, 2010. Differential expression analysis for sequence count data. Genome Biology 11: R106, <http://genomebiology.com/2010/11/10/R106>
3. Ayling, A.L., 1983. Growth and regeneration rates in thinly encrusting demospongiae from temperate waters. The Biological Bulletin 165: 343-35.
4. Bennett, H., J.J. Bell, S.K. Davy, N.S. Webster & D.S. Francis, 2018. Elucidating the sponge stress response: lipids and fatty acids can facilitate survival under future climate scenarios. Global Change Biology 2(7): 3130–3144, DOI: 10.1111/gcb.14116
5. Blunt, J.W., B.R. Copp, R.A. Keyzers, M.H.G. Munro & M.R. Prinsep, 2015. Marine Natural Products. Natural Product Reports 32: 116-211.
6. Bolger, A.M., M. Lohse & B. Usadel, 2014. Trimmomatic: a flexible trimmer for Illumina sequence data. Bioinformatics btu170.
7. Borisenko, I. E., M. Adamska, D.B. Tokina, & A.V. Ereskovsky, 2015. Transdifferentiation is a driving force of regeneration in *Halisarca dujardini* (Demospongiae, Porifera). PeerJ 3: e1211. <https://doi.org/10.7717/peerj.1211>
8. Buchfink, B., C. Xie & D.H. Huson, 2015. Fast and sensitive protein alignment using DIAMOND. Nature Methods 12(1): 59-60.
9. Conaco, C., P. Neveu, H. Zhou, M.L. Arcila, S.M. Degnan, B.M. Degnan, & K.S. Kosik, 2012. Transcriptome profiling of the demosponge *Amphimedon queenslandica* reveals genome-wide events that accompany major life cycle transitions. BMC Genomics 13: 209-228.
10. Coutinho, C.C., I. de Andrade Rosa, J.D. de Oliveira Teixeira, L.R. Andrade, M.L. Costa & C. Mermelstein, 2017. Cellular migration, transition and interaction during regeneration of the sponge *Hymeniacidon heliophila*. PLoS ONE 12(5): e0178350, doi: 10.1371/journal.pone.0178350.
11. Diehl-Seifert, B., B. Kurelec, R.K. Zahn, A. Dorn, B. Jericevic, G. Uhlenbruck & W.E.G. Muller, 1985. Attachment of sponge cells to collagen substrata: effect of a collagen assembly factor. Journal of Cell Science 79: 271-285.
12. Edgar, R., M. Domrachev & A.E. Lash, 2002. Gene Expression Omnibus: NCBI gene expression and hybridization array data repository. Nucleic Acids Research 30(1): 207-210.
13. Ehrlich, H., M. Wysokowski, S. Zółtowska-Aksamitowska, L. Petrenko & T. Jesionowski, 2018. Collagens of Poriferan Origin. Marine Drugs 16: 79. doi:10.3390/md16030079
14. Ereskovsky, A. V., I.E. Borisenko, P. Lapébie, E. Gazave, D.B. Tokina & C. Borchiellini, 2015. *Oscarella lobularis* (Homoscleromorpha, Porifera) Regeneration: Epithelial Morphogenesis and Metaplasia. PLoS One 10(8): e0134566. <https://doi.org/10.1371/journal.pone.0134566>
15. Ereskovksy, A.V., I. Boriensko, A. Lavrov, F. Bolshakov, D. Tokina, M. Adamsky & M. Adamska, 2017a. Body plan formation during regeneration in sponges. presented in 4th International Congress on Invertebrate Morphology (ICIM4) 18 – 23 August 2017 Moscow, Russia.

16. Ereskovsky, A.V., A. I. Lavrov, F.V. Bolshakov & D.B. Tokina, 2017b. Regeneration in White Sea sponge *Leucosolenia complicata*(Porifera, Calcarea). *Invertebrate Zoology* 14(2): 108–113.
17. Ereskovsky, A.V., D. J. Richter, D.V. Lavrov, K.J. Schippers & S.A. Nichols, 2017c. Transcriptome sequencing and delimitation of sympatric *Oscarella* species (*O.carmela* and *O. pearsei* sp. nov) from California, USA. *PLoS ONE* 12(9): e0183002.
18. Ereskovsky, A.V., D.B. Tokina, D.M. Saidov, S. Baghduian, E Le Goff & A.I. Lavrov, 2019. Transdifferentiation and mesenchymal-to-epithelial transition during regeneration in demospongiae (Porifera), *Journal of Experimental Zoology Part B: Molecular and Developmental Evolution* 1-22, doi: 10.1002/jez.b.22919.
19. Fortunato, S.A.V., M. Adamski, O.M. Ramos, S. Leininger, J. Liu, D.E.K. Ferrier & M. Adamska, 2014. Calcisponges have a ParaHox gene and dynamic expression of dispersed NK homeobox genes. *Nature* 514: 620-635, doi: 10.1038/nature13881.
20. Francis, W.R., M. Eitel, S. Vargas, M. Adamski, S.H.D. Haddock, S. Krebs, H. Blum, D. Erpenbeck & G. Woerheide, 2017. The genome of the contractile demosponge *Tethya wilhelma* and the evolution of metazoan neural signalling pathways. *Biorxiv* doi: <http://dx.doi.org/10.1101/120998>.
21. Grabherr, M.G., B. J. Haas, M. Yassour, J. Z. Levin, D.A. Thompson, I. Amit, X. Adiconis, L. Fan, R. Raychowdhury, Q. Zeng, Z. Chen, E. Mauceli, N. Hacohen, A. Gnirke, N. Rhind, F. di Palma, B.W. Birren, C. Nusbaum, K. Lindblad-Toh, N. Friedman & A. Regev, 2011. Full-length transcriptome assembly from RNA-Seq data without a reference genome. *Nature Biotechnology* 29(7): 644-652.
22. Grice, L.E. & B.M. Degnan, 2017. Transcriptomic profiling of the allorecognition response to grafting in the Demosponge *Amphimedon queenslandica*. *Marine Drugs* 15: 136-149.
23. Goetz, S., J.M. Garcia-Gomez, J. Terol, T.D. Williams, S.H. Nagaraj, M.J. Nueda, M. Robles, M. Talon, J. Dopazo & A. Conesa, 2008. High-throughput functional annotation and data mining with the Blast2GO suite. *Nucleic Acids Research* 36(10): 3420–3435.
24. Guzman, C. & C. Conaco, 2016. Gene expression dynamics accompanying the sponge thermal stress response. *PLoS ONE* 11(10): e0165368.
25. Henry, L. & M. Hart, 2005. Regeneration from injury and resource allocation in sponges and corals – a review. *International Review of Hydrobiology* 90(2): 125–158.
26. Hoppe, W.H., 1998. Growth, regeneration and predation in three species of large coral reef sponges. *Marine Ecology Progress Series* 50: 117-125.
27. Howe, E.A., R. Sinha, D. Schlauch & J. Quackenbush, 2011. RNA-Seq analysis in MeV. *Bioinformatics* 27(22): 3209-3210.
28. Kenny, N.J., J.M. de Goeij, D.M. de Bakker, D.M., C.G. Whalen, E. Berezikov & A. Riesgo, 2018. Towards the identification of ancestrally shared regenerative mechanisms across the Metazoa: A Transcriptomic case study in the Demosponge *Halisarca caerulea*. *Marine Genomics* 37: 135–147.
29. Larroux, C., B. Fahey, D. Liubicich, V.F. Hinman, M. Gauthier, M. Gongora, K. Green, G. Wörheide, S.P. Leys & B. Degnan, 2006. Developmental expression of transcription factor genes in a demosponge: insights into the origin of metazoan multicellularity. *Evolution & Development* 8(2): 150-173.
30. Lavrov, A.I. & I.A. Kosevich, 2014. Sponge cell reaggregation: Mechanisms and dynamics of the process. *Russian Journal of Developmental Biology* 45(4): 205-223. <https://doi.org/10.1134/S1062360414040067>
31. Lavrov, A.I. & I.A. Kosevich, 2016. Sponge cell reaggregation: Cellular structure and morphogenetic potencies of multicellular aggregates. *Journal of Experimental Zoology: Part A Ecological Genetics & Physiology* 325A: 158-177. <https://doi.org/10.1002/jez.2006>

32. Lavrov, A.I., F. V. Bolshakov, D.B. Tokina & A.V. Ereskovsky, 2018. Sewing wounds up: the epithelial morphogenesis as a central mechanism of calcareous sponge regeneration. *Journal of Experimental Zoology Part B: Molecular and Developmental Evolution* 330: 351-371. <https://doi.org/10.1002/jezb.22830>
33. Li, B. & C.N. Dewey, 2011. RSEM: accurate transcript quantification from RNA-Seq data with or without a reference genome. *BMC Bioinformatics* 12: 323.
34. Li, W. & A. Godzik, 2006. CD-HIT: a fast program for clustering and comparing large sets of protein or nucleotide sequences. *Bioinformatics* 22: 1658-1659.
35. Moriya, Y., M. Itoh, S. Okuda, A.C. Yoshizawa & M. Kanehisa, 2007. KAAS: an automatic genome annotation and pathway reconstruction server. *Nucleic Acids Research* 35: W182–W185, doi:10.1093/nar/gkm321.
36. Nichols, S.A., B.W. Roberts, D.J. Richter, S.R. Fairclough & N. King, 2012. Origin of metazoan cadherin diversity and the antiquity of the classical cadherin/ β -catenin complex. *Proceedings of the National Academy of Sciences* 109(32): 13046-13051, <https://doi.org/10.1073/pnas.1120685109>.
37. Paul, V.J., M.P. Puglisi & R. Ritson-Williams, 2006. Marine chemical ecology. *Natural Product Reports* 23 (2): 153-180.
38. Pawlik, J., B. Chanas, R. Toonen & W. Fenical, 1995. Defences of Caribbean sponges against predatory reef fish. I. Chemical deterrence. *Marine ecology Progress Series* 127 (1): 183-194.
39. Pawlik, J.R., T-L. Loh, S.E. McMurray, 2017. A review of bottom-up vs top-down control of sponges on Caribbean fore-reefs: what's old, what's new, and future directions. *PeerJ* 6: e4343, doi 10.7717/peerj.4343.
40. Perez-Porro, A.R., D. Navarro-Gomez, M.J. Uriz, & G. Giribet, 2013. A NGS approach to the encrusting Mediterranean sponge *Crella elegans* (Porifera, Demospongiae, Poecilosclerida): transcriptome sequencing, characterization and overview of the gene expression along three life cycle stages. *Molecular Ecology Resources* 13: 494-509.
41. Pozzolini, M., L. Gallus, S. Ghignone, S. Ferrando, S. Candiani, M. Bozzo, M. Bortolino, G. Costa, G. Bravestello & S. Scarfi (2019) Insights into the metazoan regenerative mechanisms: roles of TGF superfamily members in tissue regeneration of the marine sponge *Chondrosia reniformis*. *Journal of Experimental Biology* 222: jeb207894 doi:10.1242/jeb.207894.
42. Puchtler, H., F.S. Waldrop & L.S. Valentine, 1973. Polarization microscopic studies of connective tissue stained with Picro-Sirius Red FBA. *Beitrage zur Pathologie* 150: 174-187.
43. Qiu, F., S. Ding, H. Ou, D. Wang, J. Chen & M.M. Miyamoto, 2015. Transcriptome changes during the life cycle of the Red sea sponge, *Mycale phyllophila* (Porifera, Demospongiae, Poecilosclerida). *Genes* 6: 1023-1052.
44. Raine-Fenning N.J., M.P. Brincat & Y. Muscat-Baron (2003) Skin ageing and menopause: implications for treatment. *American Journal of Clinical Dermatology* 4(6): 371-378
45. Renard, E., S.P. Leys, G. Wörheide & C. Borchellini, 2018. Understanding animal evolution: the added value of sponge transcriptomics and genomics. *BioEssays* 40(9): e1700237, doi: 10.1002/bies.201700237.
46. Responde D.J., R.M. Natoli & K.A. Athanasiou (2007) Collagens of articular cartilage: structure, function, and importance in tissue engineering. *Biomedical Engineering* 35(5): 363-411
47. Riesgo, A., S.C.S. Andrade, P.P. Sharma, M. Novo, A.R. Perez-Porro, V. Vahtera, V.L. Gonzalez, G.Y. Kawauchi & G. Giribet 2012. Comparative description of ten transcriptomes

- of newly sequenced invertebrates and efficiency estimation of genomic sampling in non-model taxa. *Frontiers in Zoology* 9: 33-57.
48. Riesgo, A., N. Farrar, P.J. Windsor, G. Giribet & S.P. Leys, 2014. The analysis of eight transcriptomes from all Poriferan classes reveals surprising genetic complexity in sponges. *Molecular Biology and Evolution* 31(5): 1102-1120.
 49. Riesgo, A., K. Peterson, C. Richardson, T. Heist, B. Strehlow, M. McCauley, M. Hill & A. Hill, 2014. Transcriptomic analysis of differential host gene expression upon uptake of symbionts: a case study with *Symbiodinium* and the major bioeroding sponge *Cliona varians*. *BMC Genomics* 15: 376-398.
 50. Reiswig, H.M., 1973. Population dynamics of three Jamaican Demospongiae. *Bulletin of Marine Science* 23(2): 191-226.
 51. Schmahl, G.P., 1999. Recovery and growth of the giant barrel sponge (*Xestospongia muta*) following physical injury from a vessel grounding in the Florida Keys. *Memoires of Queensland Museum* 44: 532-532.
 52. Shield, C.J. & J.D. Witman, 1993. The impact of *Henricia sanguinolenta*(O.F. Müller) (Echinodermata:Asteroidea) predation on the finger sponges, *Isodictya* spp. *Journal of Experimental Marine Biology & Ecology* 166: 107-33.
 53. Simpson, T.L., 1984. *The cell biology of sponges*. Springer-Verlag, New York Inc.
 54. Singh, A. & N. L. Thakur, 2016. Influence of spatial competitor on the growth and regeneration of the marine sponge *Cinachyrella* cf. *cavernosa* (Porifera, Demospongiae). *Hydrobiologia* 768: 111-123.
 55. Srivastava, M., O. Simakov, J. Chapman, B. Fahey, M.E.A. Gauthier, T. Mitros, G.S. Richards, C. Conaco, M. Dacre, U. Hellsten, C. Larroux, N.H. Putnam, M. Stanke, M. Adamska, A. Darling, S.M. Degnan, T.H. Oakley, D.C. Plachetzki, Y. Zhai, M. Adamski, A. Calcino, S.F. Cummins, D.M. Goodstein, C. Harris, D.J. Jackson, S.P. Leys, S. Shu, B.J. Woodcroft, M. Vervoort, K.S. Kosik, G. Manning, B.M. Degnan & D.S. Rokhsar, 2010. The *Amphimedon queenslandica* genome and the evolution of animal complexity. *Nature* 466: 720-728, doi:10.1038/nature09201.
 56. Swatschek, D., W. Schatton, J. Kellermann, W.E.G. Mueller & J. Kreuter, 2002. Marine sponge collagen: isolation, characterization and effects on the skin parameters surface-pH, moisture and sebum. *European Journal of Pharmaceutics & Biopharmaceutics* 53: 107-113.
 57. Van Soest, R.W.M., N. Boury-Esnault, J. Vacelet, M. Dohrmann, D. Erpenbeck, N.J. De Voogd, N. Santodomingo, B. Vanhoorne, M. Kelly & J.N.A. Hooper, 2012. Global diversity of sponges (Porifera). *PLoS ONE* 7(4): e35105, doi:10.1371/journal.pone.0035105.
 58. Voigt, O., M. Adamaska, M. Adamaski, A. Kittlemann, W. Lukardis & G. Wörheide, 2017. Spicule formation in calcareous sponges: coordinated expression of biomineralization genes and spicule-type specific genes. *Scientific Reports* 7: 45658-45668.
 59. Wickham, H., 2016. *ggplot2: Elegant Graphics for Data Analysis*. Springer-Verlag New York. ISBN 978-3-319-24277-4.
 60. Wilkinson, C.R. & J.E. Thompson, 1997. Experimental sponge transplantation provides information on reproduction by fragmentation. In *Proceedings of the 8th International Coral Reef Symposium, Vol. 2*. Panama: Smithsonian Tropical Research Institute. p. 1417-20.
 61. Wulff, J.L., 2006. Resistance vs recovery: morphological strategies of coral reef sponges. *Functional Ecology* 20: 699-708.
 62. Wulff, J., 2010. Regeneration of sponges in ecological context: is regeneration an integral part of life history and morphological strategies? *Integrative and Comparative Biology* 50(4): 494-505, doi:10.1093/icb/icq100.

Fig 1 Schematic of the experimental design showing basal and apical part of the sponge *Cinachyrella cf cavernosa*

Fig 2 Wound healing pattern in *C.cf cavernosa* based on wound location showing wounds at basal region regenerating faster than those at the apical region. ggplot2 was used to plot this graph (Wickham, 2016).

Fig 3 Regeneration in *C. cf cavernosa* based on the wound location and presence of collagen. Fig 3A (a) to (c) show succession of wound healing in basal tissue of *C.cf cavernosa*. (a) day 0, (b) day 7, (c) day 10. (d) to (f) show histological sections at the respective stages, stained with Picro-Sirius red as seen under bright light. (g) to (i) show the same sections under polarised light. Here, collagen can be seen illuminated as green bands (thin collagen) and orange bands (thick collagen). Fig3B (a) to (c) show succession of wound healing in apical tissue of *C. cf cavernosa*. (a) day 0, (b) day 7, (c) day 20. (d) to (f) show corresponding histological sections under bright light. (g) to (i) show the same sections under polarised light. The collagen content in basal tissue is more than that of apical tissue. Basal tissue also contains more of thicker collagen than apical tissue

Fig 4 Transmission electron micrographs of collagen in *C. cf cavernosa*. (a) Basal tissue on day 0 (control). (b) Basal tissue on day 7 (regenerating tissue). Arrowheads show clumps of collagen starting to form. (c) Basal tissue on day 10 (completely regenerated tissue). Arrowheads show clumps of collagen. (d) Apical tissue on day 0 (control). (e) Apical tissue on day 7 (regenerating tissue). Arrowheads show clumps of collagen. (f) Apical tissue on day 20 (completely regenerated). Arrowheads show clumps of collagen.

Fig 5 Collagen extracted from the sponge sample of *C.cf cavernosa* based on wound location after complete regeneration. Basal tissue shows on an average 22% more collagen content than apical tissue. The chart was plotted using ggplot2 (Wickham, 2016)

Fig 6 Transmission electron micrographs of *C. cf cavernosa* (a) Archaeocyte - arrowhead indicates large nucleus and square-heads indicate heterogeneous inclusions; (b) Choanocytes are indicated with arrowheads, microvilli and flagellum detached from the cells can also be seen inside the choanocyte chamber; (c) Arrowheads indicate phagocytosed bacteria inside a large bacteriocyte; (d) Arrowhead indicates collagen secreting out of a collencyte; (e) Two cells with inclusions; (f) Elongated cells migrating along one axis.

Table 1 Assembly-wise CDS summary

Description	Assembly A	Assembly B	Assembly C
No. of CDS	1928	1769	2127
Total CDS length (bp)	948375	894729	1068762
Maximum CDS length	2865	5346	3942
Minimum CDS length	264	258	258
Average CDS length	431	505	502

Table 2 Top ten up-regulated and down-regulated genes between two samples					
Before wound infliction vs during regeneration - up-regulation		Before wound infliction vs complete regeneration - up-regulation		During regeneration vs complete regeneration - up-regulation	
CDS ID	Annotation	CDS ID	Annotation	CDS ID	Annotation
33347	WD repeat-containing protein 48-like	49435	Methylmalonic aciduria type A protein, mitochondrial-like	40420	Ubiquitin carboxyl-terminal hydrolase 4-like
25433	Uncharacterized protein LOC106159483	5644	Uncharacterized protein LOC109586012	60028	Xylulose kinase
38455	ATP-dependent DNA helicase PIF1-like	57573	Multidrug resistance protein 1-like	43612	ATP-dependent RNA helicase DDX3X isoform X1
25133	Hypothetical protein M514_11684	32788	AN1-type zinc finger protein 5-like	61880	Eukaryotic peptide chain release factor
49435	Methylmalonic aciduria type A protein, mitochondrial-like	45991	SH3 and PX domain-containing protein 2A-like	23574	Prostaglandin reductase 1-like
25134	Hypothetical protein M514_11684	40348	Lambda-crystallin-like	36942	Hypothetical protein TRIADDRAFT_20956
888	Hypothetical protein TRFO_12271	11910	Rab2	25869	Glutaredoxin-1-like
3917	PiggyBac transposable element-derived protein 5	33347	WD repeat-containing protein 48-like	50967	Cystathionine gamma-lyase-like
35193	CLK4-associating serine/arginine-rich protein-	60280	Protein unc-13 homolog D-like	53397	Uncharacterized protein LOC109588626

	like isoform X1				
32296	Receptor-type tyrosine-protein phosphatase epsilon-like	6351	Endothelial PAS domain-containing protein 1-like	21700	Col protein
Before wound infliction vs during regeneration - down-regulation		Before wound infliction vs complete regeneration - down-regulation		During regeneration vs complete regeneration - down-regulation	
CDS ID	Annotation	CDS ID	Annotation	CDS ID	Annotation
43612	ATP-dependent RNA helicase DDX3X isoform X1	16596	Histidine--tRNA ligase, cytoplasmic-like	13032	PiggyBac transposase Uribo1
40420	Ubiquitin carboxyl-terminal hydrolase 4-like	49741	Dynein beta chain, ciliary-like	888	Hypothetical protein TRFO_12271
6598	Hypothetical protein B6247_26100	39433	L14 ribosomal protein	45076	Uncharacterized protein LOC109473188
51548	Dynein light chain Tctex-type 1	45134	Pygopus homolog 2-like	41618	Alanine--glyoxylate aminotransferase 2-like
31887	Erythrocyte band 7 integral membrane protein-like	16444	L2/L8 ribosomal protein	6623	Transposable element Tcb2 transposase
63357	Plasminogen activator inhibitor 1 RNA-binding protein-like	24583	Keratin-associated protein 5-3-like	30679	Zinc finger BED domain-containing protein 4-like
792	FACT complex subunit Ssrp1-like	31887	Erythrocyte band 7 integral membrane	27764	Transcriptional repressor NF-X1 isoform

			protein-like		X3
23574	Prostaglandin reductase 1-like	3781	40S ribosomal protein S10-like	33347	WD repeat-containing protein 48-like
25798	RNA-binding protein 25-like	13284	Peptidyl-tRNA hydrolase ICT1, mitochondrial-like	8103	Ras-related protein RABD2c
36334	mKIAA1323 protein	63357	Plasminogen activator inhibitor 1 RNA- binding protein-like	61151	PiggyBac transposable element-derived protein 4-like

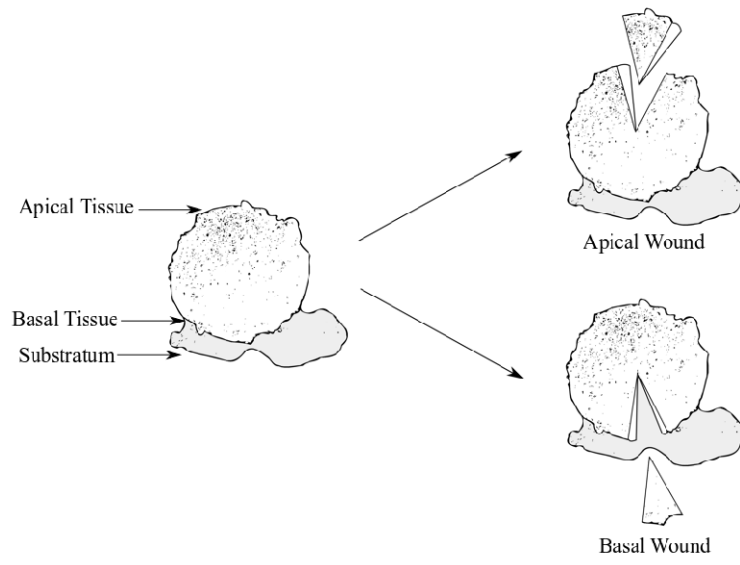


Figure 1

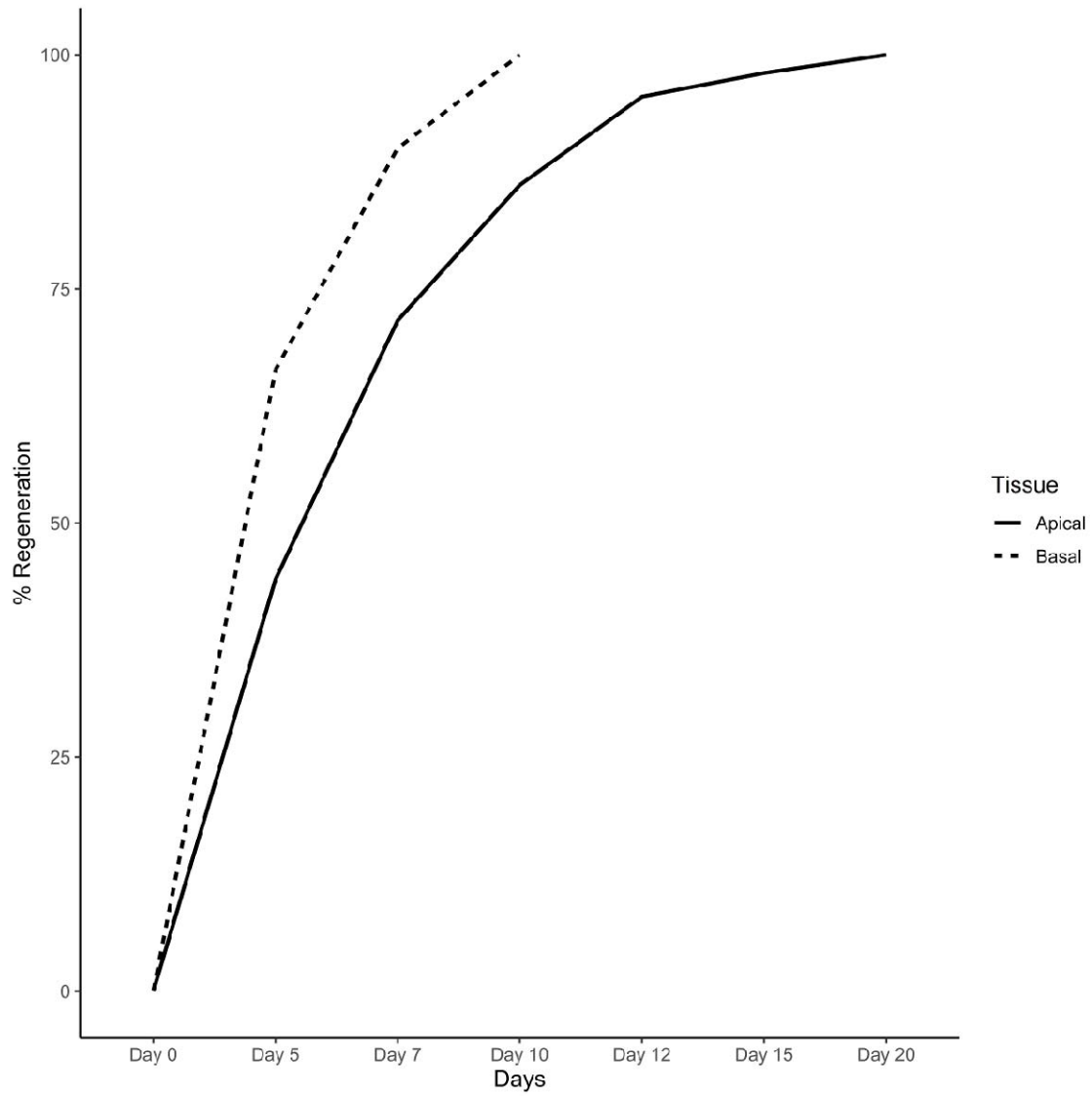


Figure 2

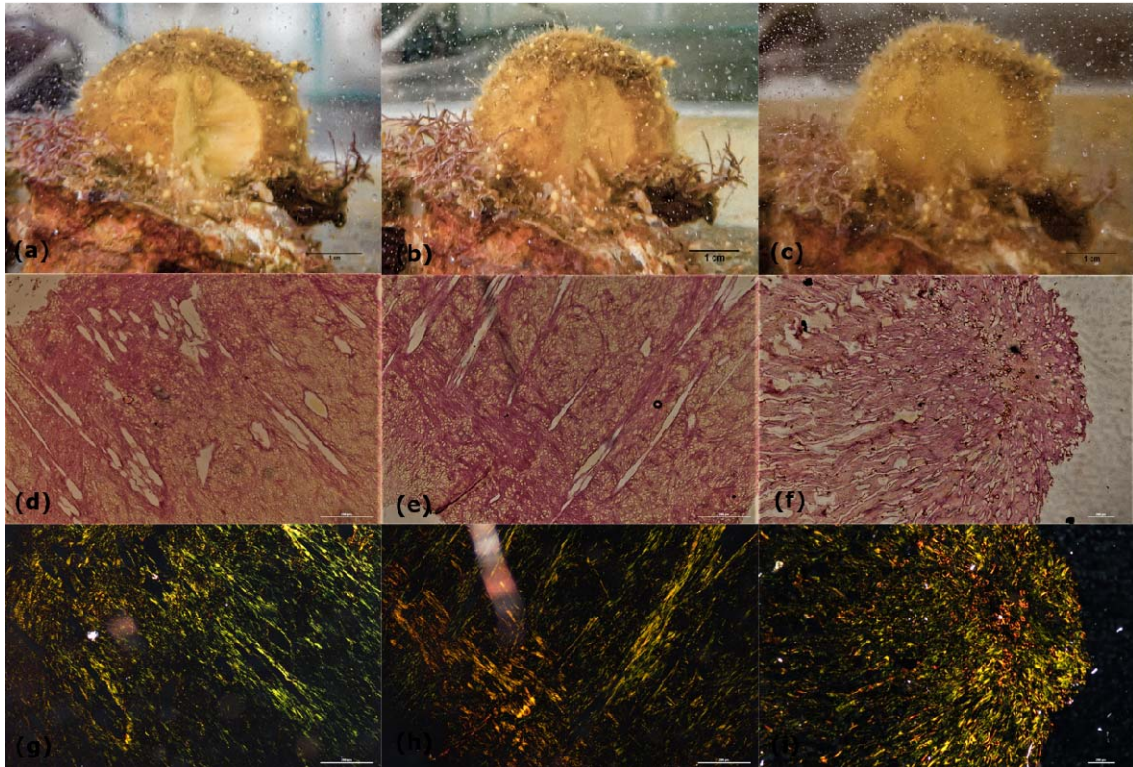


Figure 3A

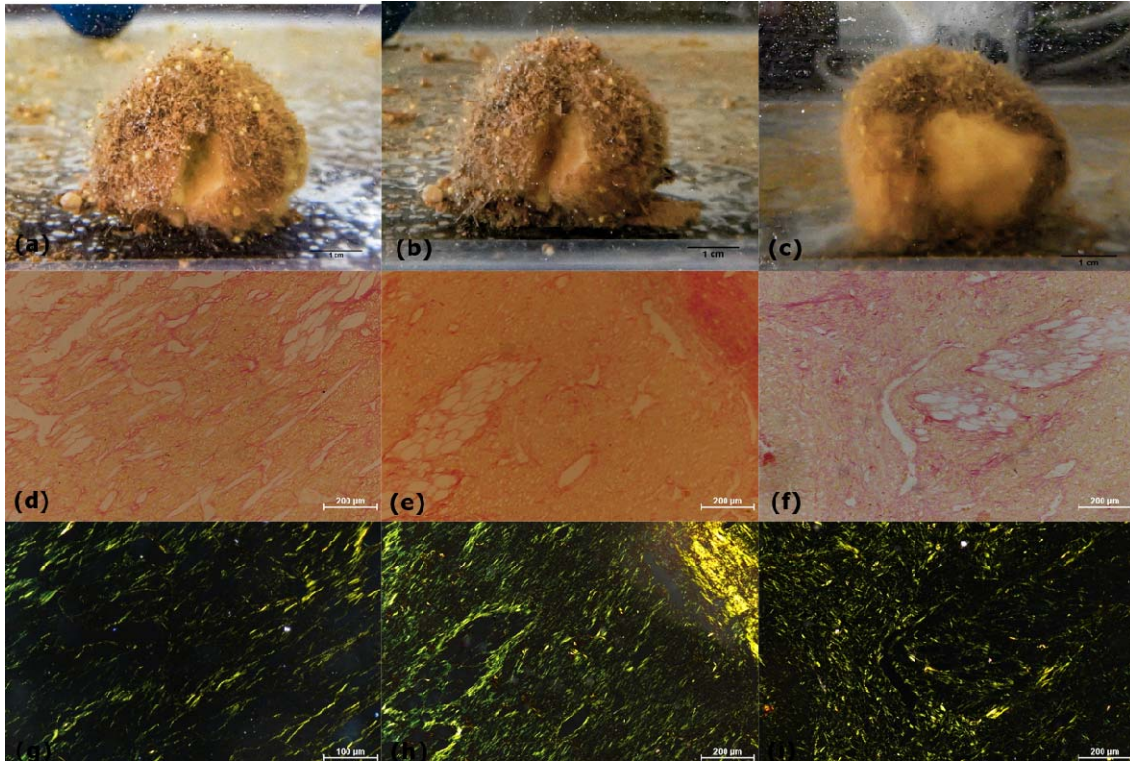


Figure 3B

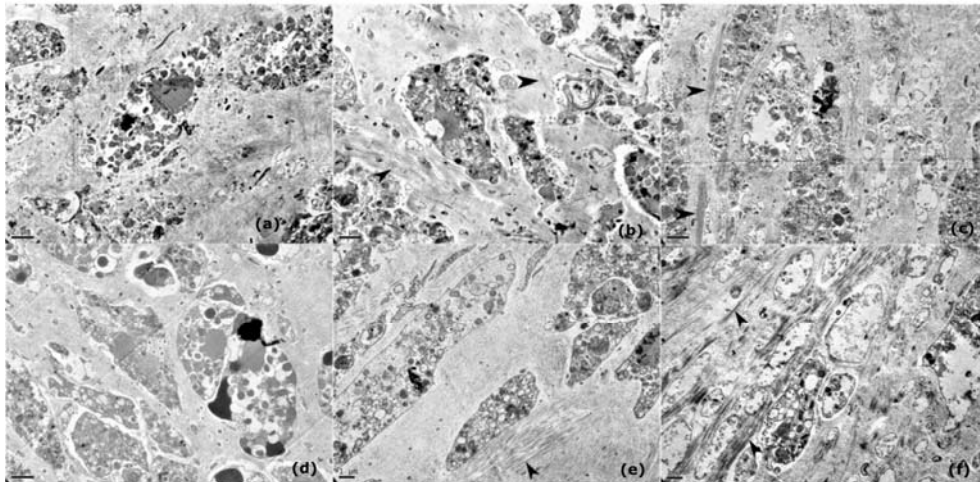


Figure 4

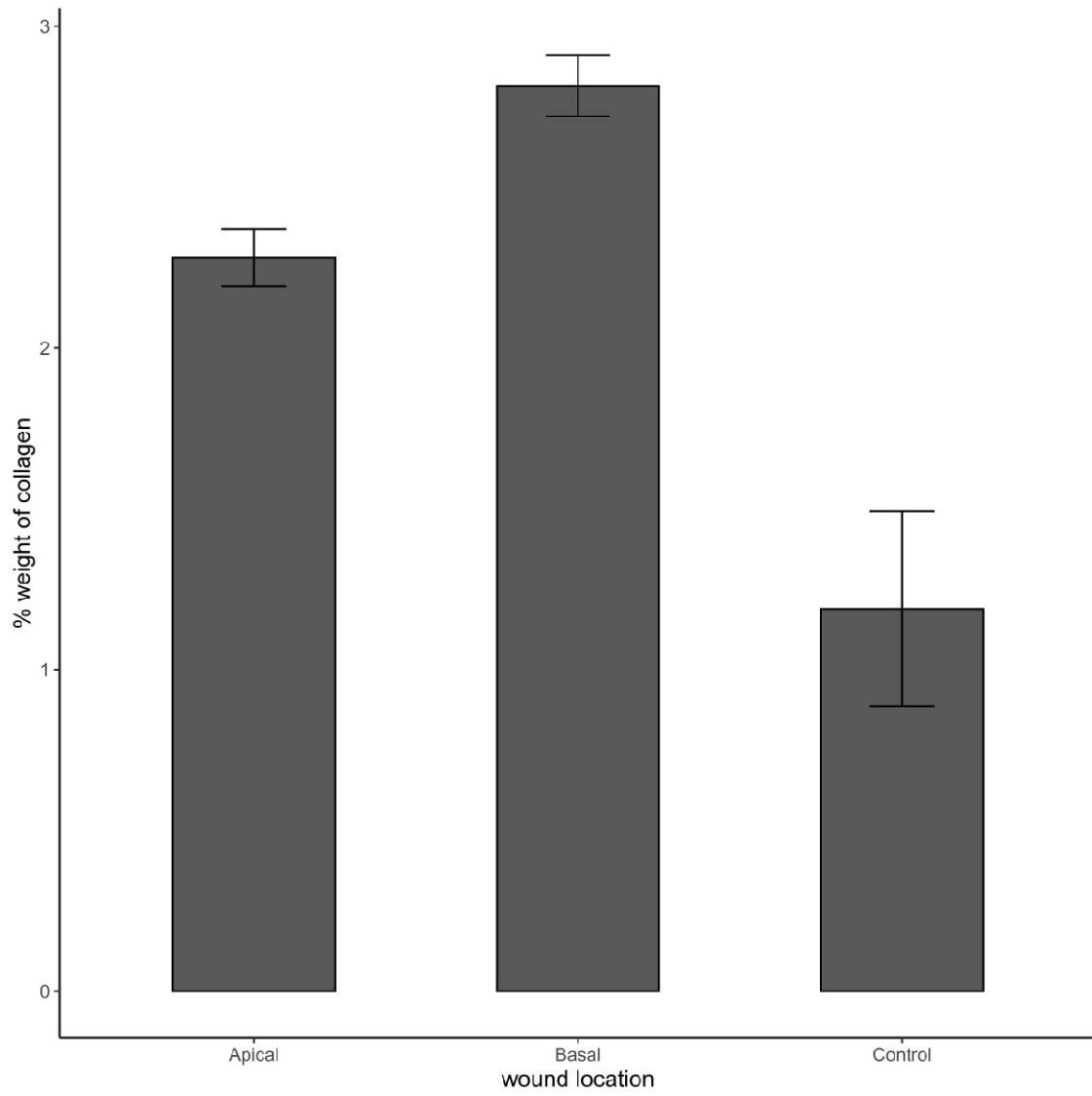


Figure 5

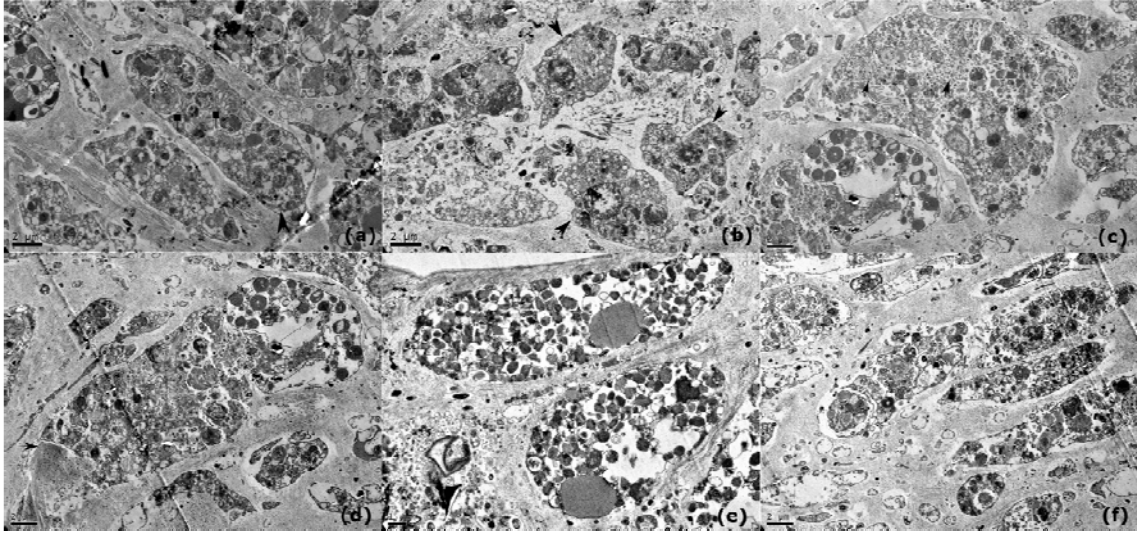


Figure 6